

PREDICTION OF MULTI-TARGET DYNAMICS USING DISCRETE DESCRIPTORS: AN INTERACTIVE APPROACH

Mohamad Baydoun, Damian Campo, Divya Kanapram, Lucio Marcenaro, Carlo S. Regazzoni

DITEN, University of Genoa, Italy.

ABSTRACT

We propose a probabilistic method to track and interpret the interactions of moving objects. The proposed method is based on the analysis of location data from different moving objects that modify their dynamics according to rules of interactions, namely attractive and repulsive forces governing objects' motions in a scene. Our method uses a Bayesian structure to identify key elements of the interplay rules and facilitates the prediction of objects' dynamics as an interacting system. Such a prediction facilitates the detection of abnormalities by identifying unseen interaction effects in the scene.

Index Terms— Abnormality detection, interacting models, trajectory analysis, Kalman filter, Particle filter.

1. INTRODUCTION

Modeling and understanding trajectories are important tasks for intelligent transportation [1, 2], surveillance [3, 4, 5] and autonomous systems [6, 7, 8]. Moving objects can be modeled as a series of interactions with their surroundings such that their dynamics are a result of forces (external effects) that act on them over time [9]. The first attempt to understand human trajectories based on force field models explains the motion of individuals in simulations as an effect produced by surrounding structures and other pedestrians [10]. Other works apply such concepts in real scenarios [11, 12] and generalize the formulation to other kinds of applications, such as people re-identification [13], group detection [14] and other objects different from pedestrians [9].

Forces that act over objects can be attractive or repulsive. Goals, i.e., destination points, can be represented by attractive forces and obstacles, i.e., structures or other entities, as repulsive forces [13, 15]. Accordingly, a trajectory can be explained by the combination of different forces that operate on the moving object. By identifying and modeling attractive/repulsive forces produced by constituent parts of the environment, we can build complex models that explain the interplay between objects and their surroundings. We aim to model such interactions in a probabilistic manner through a Dynamic Bayesian Network (DBN) structure. DBNs have been used for representing temporal relationships of systems that evolve through time. It is the case of predictive models based on objects' locations and their time derivatives [16, 17, 18, 19] or detection of abnormalities [20, 21, 22]. Our method is based on a DBN approach that facilitates the characterization of objects' dynamics and their inter-dependencies. In turn, our approach enables the detection of abnormalities concerning previous observations. Anomalies are interpreted as new force fields that interact with moving objects. In this work, interactions are simulated as a set of rules based on force fields; observed data facilitates to explain those interactions as probabilistic inferences caused by the activation of switching variables

in a DBN. In order to build such DBN, we first create a vocabulary of spatial zones in a scene where constant velocity patterns are valid based on multiple observed objects. To this end, we employ a baseline Kalman Filter (KF) that generates familiar objects' displacements based on their position in the environment.

Then, we use transitions between the zones to track newly observed objects by employing a set of KFs, which model the behaviors of continuous variables. Moreover KFs are coupled with a particle filter (PF) method which describes the evolution of discrete variables under an assumption of interaction. Finally, we employ probabilistic abnormality indicators to detect unseen behaviors in the dynamic interplay between objects.

This paper is motivated by previous works on encoding static force field information based on moving data [23] and inference of states/superstates abnormalities in trajectory data [24]. Nonetheless, this paper differs from previous works since *i)* It presents a novel way for modeling conditional dependencies between couples of observed objects. *ii)* It employs a coupled DBN structure that connects information of moving interacting objects. *iii)* Inferences from the proposed coupled DBN are used to detect abnormalities of each object depending on the state of their surroundings. Simulated data is employed for validating the DBN performance at the coding force field interacting rules into probabilistic models.

The rest of the paper is divided as follows: Section 2 presents the proposed method for modeling interactions between moving objects. Section 3 shows the obtained results in simulated data. Section 4 concludes the article and proposes some future works.

2. PROPOSED METHOD

Let Z_k^1 and Z_k^2 be the observed positions of two entities, namely *object 1* and *object 2*. Both entities are assumed to interact with each other at a given time instant k . Let us consider a KF which uses zero order motion dynamical equation:

$$\tilde{X}_{k+1} = A\tilde{X}_k + w_k, \quad (1)$$

where \tilde{X}_k represents the object's state composed of its generalized coordinate positions and their respective velocities in a time instant k , such that $\tilde{X}_k = [\mathbf{x} \ \dot{\mathbf{x}}]^\top$. $\mathbf{x} \in \mathbb{R}^d$ and $\dot{\mathbf{x}} \in \mathbb{R}^d$. d represents the number of coordinates of the environment. $A = [A_1 \ A_2]$ is a dynamic model matrix: $A_1 = [I_d \ 0_{d,d}]^\top$ and $A_2 = 0_{2d,d}$. I_n represents a square identity matrix of size n and $0_{l,m}$ is a $l \times m$ null matrix. w_k represents the prediction noise which is here assumed to be zero-mean Gaussian for all variables in X_k with a covariance matrix Q , such that $w_k \sim \mathcal{N}(0, Q)$. As can be seen from the equation (1), the proposed model suggests that moving objects will rest in a quasi-static location and only random noise perturbations, modeled by w_k will affect their states. The linear relationship between

measurements and the state of individuals is defined as:

$$Z_k = H\tilde{X}_k + v_k, \quad (2)$$

where $H = [I_d \ 0_{d,d}]$ is an observation matrix that maps states onto observations and v_k represents the measurement noise produced by the sensor device which is here assumed to be zero-mean Gaussian with a covariance matrix R , such that, $v_k \sim \mathcal{N}(0, R)$. By considering the dynamical filter in equation (1), it is possible to estimate the velocity by using KFs' innovations, such that:

$$v_k = \frac{Z_k - H\hat{X}_{k+1|k}}{\Delta k} \quad (3)$$

where $\hat{X}_{k+1|k}$ is the state space estimation of the time instant $k+1$ given observations until time k . Δk is the sampling time.

In this paper, two independent unmotivated KFs are applied synchronously to position data of *object 1* and *object 2*. A joint state space vector (System generalized states) is defined as \tilde{X}_k and consists of both state object's state at each time instant k , such that:

$$\tilde{X}_k = \begin{bmatrix} \tilde{X}_k^1 \\ \tilde{X}_k^2 \end{bmatrix}, \quad (4)$$

where \tilde{X}_k^1 and \tilde{X}_k^2 represent the generalized states of *object 1* and *object 2* respectively.

2.1. Training phase (learning a DBN)

After obtaining a set of generalized joint states coming from training examples that describe a specific type of interaction between moving objects, it is proposed to perform a training phase whose objective consists in learning a switching DBN, see Fig.1, for modeling and predicting the interactive dynamical system over time. Four steps to learn the switching DBN are done, such that:

Learn vocabularies and dictionary. A discretization of the state space data \tilde{X}_k is performed. Two vocabularies (one per object) are learned by using a self-organizing map (SOM) algorithm [25]. SOMs receive \tilde{X}_k data and produce a set of $4d$ -dimensional discrete variables (neurons). We use two weights, β and α : where $\alpha > \beta$ and $\beta + \alpha = 1$. The first SOM favors the velocity (action) components of *object 1*, α is associated with such component and β is distributed to the rest of the data. Similarly, the second SOM favors the velocity (action) components of *object 2* (α components), β is distributed to the rest of the data. Each SOM generates a vocabulary composed of a set of prototypes where \tilde{X}_k data is clustered. Each prototype represents a region where quasi-linear models are valid. Vocabularies are defined as:

$$S^i = \{s_1^i, s_2^i, \dots, s_{L_i}^i\}, \quad (5)$$

where L_i is the total number of prototypes associated with the *object i*. s_l^i indexes the cluster of generalized joint states that favors the *object i*'s motion. Additionally, let $\xi_{s_l^i}$ be the centroid, i.e., cluster estimation vector, containing the $4d$ -dimensional system's data represented by the cluster s_l^i .

It is proposed weighted distance to calculate the closest prototype to each joint state \tilde{X}_k , such that:

$$S_k^i = \arg \min (d_i(\tilde{X}_k, S^i)), \quad (6)$$

where $S_k^i \in S^i$. $d(\cdot, \cdot)$ is a weighted distance function between two $2d$ -dimensional vectors. Such function considers the same parameters β and α with which the SOM is trained, such that:

$$d_i(\mathcal{X}, \mathcal{Y}) = \sqrt{(\mathcal{X} - \mathcal{Y})^\top \Phi_i (\mathcal{X} - \mathcal{Y})}, \quad (7)$$

where \mathcal{X} and \mathcal{Y} are both $2d$ -dimensional vectors consisting of position and velocity components. By using equation (7), it is possible to associate the current joint state of objects with the closer discrete value from obtained SOMs. In the case of two objects, Φ_1 and Φ_2 can be written as:

$$\Phi_1 = \begin{bmatrix} \beta I_d & 0_{d,d} & 0_{d,2d} \\ 0_{d,d} & \alpha I_d & 0_{d,2d} \\ 0_{2d,d} & 0_{2d,d} & \beta I_{2d} \end{bmatrix}; \Phi_2 = \begin{bmatrix} \beta I_{3d} & 0_{3d,d} \\ 0_{d,3d} & \alpha I_d \end{bmatrix}.$$

In a time instant k , each considered object i is represented by a prototype $S_k^i \in S^i$. Active prototypes from different objects are considered together as an activated word. For the case of two objects, $i \in \{1, 2\}$, the activated word at the time instant k is written as $D_k = [S_k^1, S_k^2]^\top$. Consequently, it is possible to define a dictionary containing possible couples of activated letters, such that:

$$D = \{D^1, D^2, \dots, D^M\}, \quad (8)$$

where D^m encodes a given identified word, M represents the total number of words (letter combinations); and $D_k \in D$. As can be seen, words are created based on the different prototypes activated at the same time instant. D defines the whole system's discretization.

Learn discrete transition models. By observing the activated words over time. It is possible to estimate a set of temporal transition matrices that encode the probabilities of passing from a current word to another one. Such matrices take into consideration the time spent in the current word for encoding transition probabilities, facilitating the estimation of $p(D_k | D_{k-1}, t_k)$, where t_k encodes the time spent in the current word D_{k-1} .

Regions properties. A region S_k^i is represented by the variables $\xi_{S_k^i}$, $Q_{S_k^i}$ and $\psi_{S_k^i}$, which encode respectively the mean value, the covariance matrix of clustered states and a threshold value where linear models are valid. By considering the threshold value $\psi_{s_l^i}$ as a distance from the mean superstates values $\xi_{s_l^i}$, it is possible to define a certainty boundary where the proposed models are valid. Such a threshold is defined at the letters' level as:

$$\psi_{s_l^i} = 3 * \sqrt{\text{tr}(Q_{s_l^i})}, \quad (9)$$

where $\text{tr}(\cdot)$ represents the trace operator and $Q_{s_l^i}$ is the covariance matrix of the region $s_l^i \in S^i$ calculated based on training data that falls in it.

Learn continuous models. This work expresses the evolution in time of objects state based on quasi-constant velocity models. Such type of motion can be written as a function of the previously obtained regions S^i , such that:

$$\tilde{X}_{k+1}^i = A\tilde{X}_k^i + BU_{S_k^i} + w_k, \quad (10)$$

where $B = [I_d \Delta k \ I_d]^\top$ is a control input model that maps objects' actions (velocity estimations, see equation (3)) into following states. d is the number of dimensions of trajectory data and I_n is an identity matrix of dimension n . $i \in \{1, 2\}$ indexes the objects involved in the interaction. The variable $U_{S_k^i}$ is a control vector that encodes the object's action when it is inside a region S_k^i , such that:

$$U_{S_k^i} = [\dot{x}_{S_k^i} \ \dot{y}_{S_k^i}]^\top, \quad (11)$$

where $\dot{x}_{S_k^i}$ and $\dot{y}_{S_k^i}$ are a sub-part of the centroid $\xi_{S_k^i}$ related to velocity components of object i . The transition model shown in equation (10) corresponds to a motivated dynamics whose effects are encoded in $U_{S_k^i}$ and switched according to the activated region S_k^i .

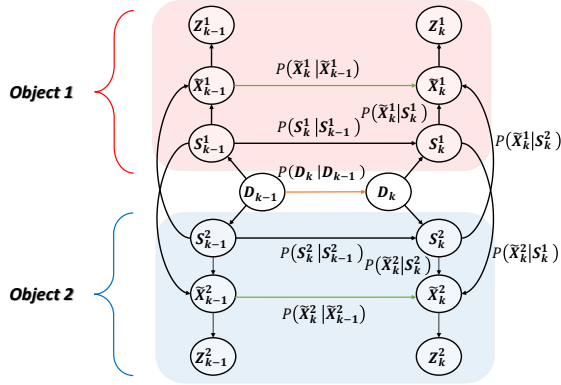


Fig. 1: A switching DBN for interactive system. Arrows represent conditional probabilities between the involved variables. Vertical arrows facilitate to describe causalities between both, continuous and discrete levels of inference and observed measurements. Horizontal arrows explain temporal causalities between hidden variables. In particular, orange arrow encodes the interaction of couples of objects and green arrows represent the influence at a continuous level

2.2. Testing phase (Online interaction tracking)

To make inferences by employing the learned DBN, see Fig.1, we use a probabilistic switching model called Markov Jump Particle filter (MJPF) [24]. Such filter uses a PF for inferring systems' discrete levels. Additionally, each considered particle employs a KF in that tracks the generalized states of observed entities. In [24], the filter is used to predict behaviors of single objects without considering the effects of other entities on their motions. Here, we employ MJPF to predict the interaction between couples of objects.

Each object has two inference levels: *i)* A continuous level, where states are inferred based on measurements (green arrows). Predictions of the type $p(\tilde{X}_k^i | \tilde{X}_{k-1}^i)$ are performed by considering a bank of KFs built according to detected zones S_k^i where quasi-constant innovations are valid, see equation (10). *ii)* A discretization of the state space, where discrete estimations of the type $p(D_k | D_{k-1})$ are computed by a particle filter. The relationship between both levels is done by using the particle filter's estimations for choosing KF models.

MJPF models the evolution in time of objects' states based on a set of particles distributed according to obtained measurements. Each particle is used for estimating future states by using a KF that uses a quasi-constant velocity model. Particles that generate low KF prediction error are propagated to the following time step. KFs' dynamical models are written in terms of the current particle region, see equation (10) and (11).

2.3. Abnormality measurement

This work proposes an abnormality measurement based on the Hellinger distance [26] between predicted coupled generalized states $p(\tilde{X}_k^i | \tilde{X}_{k-1}^i)$ and the evidence $p(Z_k^i | \tilde{X}_k^i)$, such that:

$$\theta_k^i = \sqrt{1 - \lambda_k^i}, \quad (12)$$

where

$$\lambda_k^i = \int \sqrt{p(\tilde{X}_k^i | \tilde{X}_{k-1}^i) p(Z_k^i | \tilde{X}_k^i)} d\tilde{X}_k^i. \quad (13)$$

As can be seen, for the case of $i \in \{1, 2\}$, two different abnormality measurements are obtained at each time instant k . It is relevant to note that values of λ_k^i close to 0 indicate that observations match with predictions; whereas values close to 1 reveal the presence of an abnormality.

3. RESULTS

For validating the proposed method, it is considered a set of simulated data where a moving object, here called *follower*, chases another object, here named *attractor*. In training data, the motion of the follower is described by the velocity field shown in equation (14).

$$\vec{v}_f = \left(\psi + \frac{r^2}{\phi}\right) \hat{r} + \omega, \quad (14)$$

where r represents the distance between both objects. ψ encodes the final speed with which the follower reaches the attractor. ϕ models the changes of follower's speed while it approaches the attractor. \hat{r} is a unit vector that points at the attractor's location. $\omega \sim \mathcal{N}(0, \zeta)$.

The attractor motions consist of a horizontal dynamics along the x axis at a fixed height point y_{att} . Accordingly, the attractor can move in two senses: right or left inside the interval $[x_{att}^{(min)}, x_{att}^{(max)}]$. The attractor's dynamics is a continuous motion in one sense until it reaches an interval boundary, then, it starts moving in the opposite sense covering only the defined interval points. The speed of attractor movements is defined as $|\vec{v}_a| = \Psi |\vec{v}_f|$, where $\Psi \in [0, 1]$ which guarantees that the follower reaches the attractor.

For learning a DBN structure, it is used attractor-follower data that follow the rules described previously. The following parameters are employed for simulation purposes: $\psi = 0.85$, $\phi = 700$, $\zeta = 0.1$, $\Psi = 0.75$, $y_{att} = 12$, $x_{att}^{(min)} = -15$ and $x_{att}^{(max)} = 15$. Results related to the capabilities of detecting abnormalities and encoding interacting rules are explained in detail as follows.

Abnormality detection. Testing trajectories are employed to detect abnormalities. Such new trajectories could follow exactly the same rules with which the DBN has been trained or they could contain some changes induced to the presence of a static repulsive located in the center of the scene. Accordingly, Fig.5a and Fig.5b show normal (data that follows training set rules) and abnormal scenarios respectively. In both plots, red and blue arrows represent the trajectories of follower and attractor objects. The final position of the attractor, i.e., when the follower reaches it, is displayed as a green circle. The repulsive object is plotted as a yellow circle in Fig.5b.

Figs. 2 and 3 show the result of abnormality detection in case of normal and abnormal interactions, Figs. 5a and 5b correspondingly. As can be seen in Fig. 2, we have a low abnormality (less than 0.1), which suggests that learned DBN understands the interacting rules of the simulator. From Fig. 3, it is possible to see how high abnormality values are present in the initial portion of the trajectory data, such behavior (yellow background) is due to the repulsive object's effects which alters the learned interaction model. Once the follower overpasses the obstacle, measurements of abnormality goes down (blue background), indicating that the follower-attractor interact according to the previously learned rules.

Evaluation DBN. As the ground truth of simulated rules is available, it is provided a visual comparison between theoretical velocity fields and DBN motion estimations for different attractor-follower configurations. Fig. 4 provides a qualitative comparison between theoretical velocity fields generated based on equation (14) and the corresponding prediction of the proposed DBN. Green circles represent the position of the attractor and arrows represent its

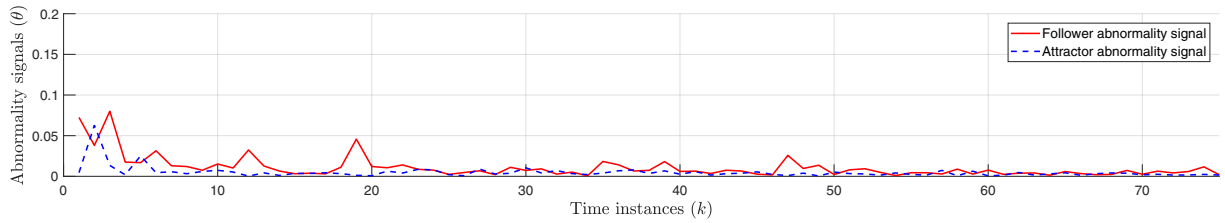


Fig. 2: Results for normal objects' interaction

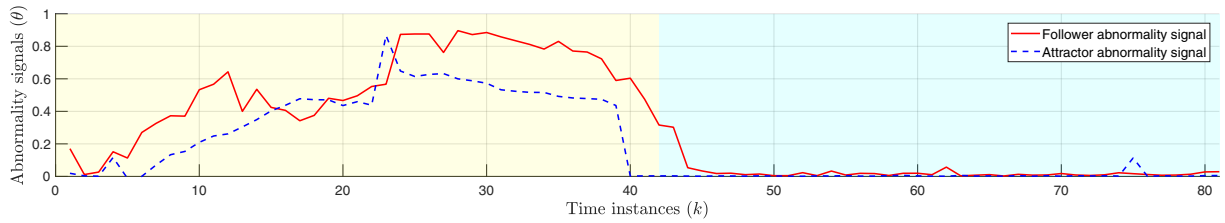


Fig. 3: Results for abnormal objects' interaction

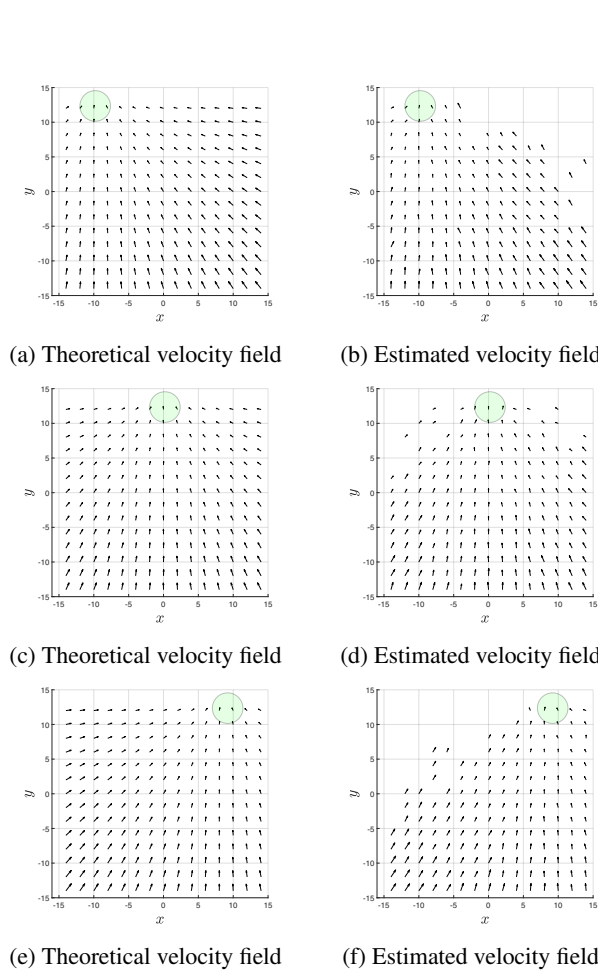


Fig. 4: Theoretical and estimated velocity fields

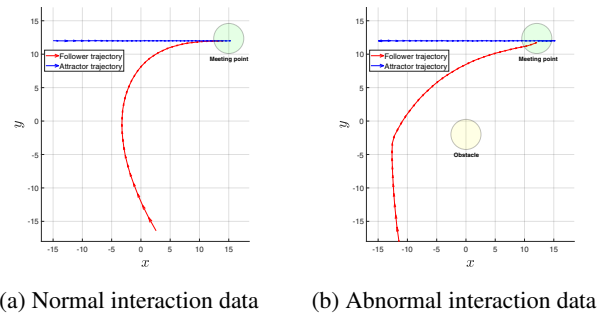


Fig. 5: Trajectories of interacting objects

generated velocity field. Empty spaces in DBN estimated fields are points where the proposed method is not able to make predictions due to lack of evidence data in such areas.

4. CONCLUSIONS

In this paper, we proposed a method for modeling interactions between moving objects. Proposed algorithms were analyzed and tested by employing simulating data.

Results suggest that attractive and repulsive forces can be modeled inside a DBN structure that codifies the normal behavior of observed objects. Continuous and discrete variables are modeled by a particle filter technique that uses a set that a set KFs that enable to detect anomalies in different inference levels in an online fashion.

Our method demonstrated the capability to encode the interactions of objects and employs such information for detecting anomalies due to previously unseen forces. Qualitative comparisons between the simulated and encoded DBN interaction rules are provided, demonstrating that the proposed models are capable of encoding observed behaviors into probability distributions. Possible future works include characterizing more complex interactions where more forces/objects are involved and understand the interplay of real moving objects inside DBN structures.

5. REFERENCES

- [1] X.C. Liu, J. Taylor, R.J. Porter, and R. Wei, "Using trajectory data to explore roadway characterization for bikeshare network," *Journal of Intelligent Transportation Systems: Technology, Planning, and Operations*, vol. 22, no. 6, pp. 530–546, 2018.
- [2] W. Jiang, J. Lian, M. Shen, and L. Zhang, "A multi-period analysis of taxi drivers' behaviors based on gps trajectories," in *2017 IEEE 20th International Conference on Intelligent Transportation Systems (ITSC)*, Oct 2017, pp. 1–6.
- [3] R. W. S. Lim, C. W. Cheong, J. See, I. K. T. Tan, L. K. Wong, and H. Q. Khor, "On vehicle state tracking for long-term carpark video surveillance," in *2017 IEEE International Conference on Signal and Image Processing Applications (IC-SIPA)*, Sept 2017, pp. 368–373.
- [4] M. Y. Choong, L. Angeline, R. K. Y. Chin, K. B. Yeo, and K. T. K. Teo, "Vehicle trajectory clustering for traffic intersection surveillance," in *2016 IEEE International Conference on Consumer Electronics-Asia (ICCE-Asia)*, Oct 2016, pp. 1–4.
- [5] J. C. Nascimento, M. A. T. Figueiredo, and J. S. Marques, "Trajectory classification using switched dynamical hidden markov models," *IEEE Transactions on Image Processing*, vol. 19, no. 5, pp. 1338–1348, May 2010.
- [6] W. Lim, S. Lee, M. Sunwoo, and K. Jo, "Hierarchical trajectory planning of an autonomous car based on the integration of a sampling and an optimization method," *IEEE Transactions on Intelligent Transportation Systems*, vol. 19, no. 2, pp. 613–626, Feb 2018.
- [7] D. Fassbender, B. C. Heinrich, T. Luettel, and H. J. Wuen-sche, "An optimization approach to trajectory generation for autonomous vehicle following," in *2017 IEEE/RSJ International Conference on Intelligent Robots and Systems (IROS)*, Sept 2017, pp. 3675–3680.
- [8] M. Baydoun, M. Ravanbakhsh, D. Campo, P. Marin, D. Martin, L. Marcenaro, A. Cavallaro, and C. S. Regazzoni, "a multi-perspective approach to anomaly detection for self-aware embodied agents," in *2018 IEEE International Conference on Acoustics, Speech and Signal Processing (ICASSP)*, April 2018, pp. 6598–6602.
- [9] D. Campo, A. Betancourt, L. Marcenaro, and C. Regazzoni, "Static force field representation of environments based on agents nonlinear motions," *Eurasip Journal on Advances in Signal Processing*, vol. 2017, no. 1, 2017.
- [10] Dirk Helbing and Peter Molnar, "Social force model for pedestrian dynamics," *Physical Review E*, vol. 51, 05 1998.
- [11] S. Seer, C. Rudloff, T. Matyus, and N. Brändle, "Validating social force based models with comprehensive real world motion data," 2014, vol. 2, pp. 724–732, The Conference on Pedestrian and Evacuation Dynamics 2014 (PED 2014), 22-24 October 2014, Delft, The Netherlands.
- [12] A. Corbetta, A. Muntean, and K. Vafayi, "Parameter estimation of social forces in pedestrian dynamics models via a probabilistic method," *Mathematical Biosciences and Engineering*, vol. 12, no. 2, pp. 337–356, 2015.
- [13] R. Mazzon and A. Cavallaro, "Multi-camera tracking using a multi-goal social force model," *Neurocomputing*, vol. 100, pp. 41–50, 2013.
- [14] R. Mazzon, F. Poiesi, and A. Cavallaro, "Detection and tracking of groups in crowd," 2013, pp. 202–207.
- [15] Xu Chen, Martin Treiber, Venkatesan Kanagaraj, and Haiying Li, "Social force models for pedestrian traffic state of the art," *Transport Reviews*, pp. 1–29, 2017.
- [16] Feng Yu, Sun Jian, and Chen Peng, "Vehicle trajectory reconstruction using automatic vehicle identification and traffic count data," *Journal of Advanced Transportation*, vol. 49, no. 2, pp. 174–194.
- [17] X. Sun, N. H. C. Yung, and E. Y. Lam, "Unsupervised tracking with the doubly stochastic dirichlet process mixture model," *IEEE Transactions on Intelligent Transportation Systems*, vol. 17, no. 9, pp. 2594–2599, Sept 2016.
- [18] G. Xie, H. Gao, L. Qian, B. Huang, K. Li, and J. Wang, "Vehicle trajectory prediction by integrating physics- and maneuver-based approaches using interactive multiple models," *IEEE Transactions on Industrial Electronics*, vol. 65, no. 7, pp. 5999–6008, July 2018.
- [19] J. C. Nascimento, M. A. T. Figueiredo, and J. S. Marques, "Activity recognition using a mixture of vector fields," *IEEE Transactions on Image Processing*, vol. 22, no. 5, pp. 1712–1725, May 2013.
- [20] X. Wang, K.T. Ma, G.-W. Ng, and W.E.L. Grimson, "Trajectory analysis and semantic region modeling using a nonparametric bayesian model," in *2008 IEEE Conference on Computer Vision and Pattern Recognition*, June 2008, pp. 1–8.
- [21] K. Kang, W. Liu, and W. Xing, "Motion pattern study and analysis from video monitoring trajectory," *IEICE Transactions on Information and Systems*, vol. E97-D, no. 6, pp. 1574–1582, 2014.
- [22] L. Chen, H. Guo, X. Wu, W. Feng, and X. Chen, "Detecting anomaly based on time dependence for large scenes," in *2016 IEEE International Conference on Information and Automation (ICIA)*, Aug 2016, pp. 1376–1381.
- [23] D. Campo, V. Bastani, L. Marcenaro, and C. Regazzoni, "Incremental learning of environment interactive structures from trajectories of individuals," in *2016 19th International Conference on Information Fusion (FUSION)*, July 2016, pp. 589–596.
- [24] M. Baydoun, D. Campo, V. Sanguineti, Lucio Marcenaro, A. Cavallaro, and Carlo S. Regazzoni, "Learning switching models for abnormality detection for autonomous driving," in *21st International Conference on Information Fusion, FUSION 2018, Cambridge, UK, July 10-13, 2018*, 2018, pp. 2606–2613.
- [25] T. Kohonen, *Self-Organizing Maps*, Physics and astronomy online library. Springer Berlin Heidelberg, 2001.
- [26] Rodolfo Lourenzutti and Renato A. Krohling, "The hellinger distance in multicriteria decision making: An illustration to the topsis and todim methods," *Expert Syst. Appl.*, vol. 41, no. 9, pp. 4414–4421, July 2014.